Biophysical Journal, Volume *110*

Supplemental Information

Three-Dimensional Structures of Full-Length, Membrane-Embedded Human $\alpha_{IIb}\beta_3$ Integrin Complexes

Xiao-Ping Xu, Eldar Kim, Mark Swift, Jeffrey W. Smith, Niels Volkmann, and Dorit Hanein

Three-dimensional structures of full-length, membrane-embedded human $\alpha_{IIb}\beta_3$ integrin complexes

X.P. Xu[1], E. Kim[1], M. Swift[1], J.W. Smith[2], N. Volkmann[1], D. Hanein[1]

[1] Bioinformatics and Structural Biology Program, Sanford Burnham Prebys Medical Discovery Institute, La Jolla, CA, USA

[2] Infectious Disease Program, Sanford Burnham Prebys Medical Discovery Institute, La Jolla, CA, USA

Supplementary Material

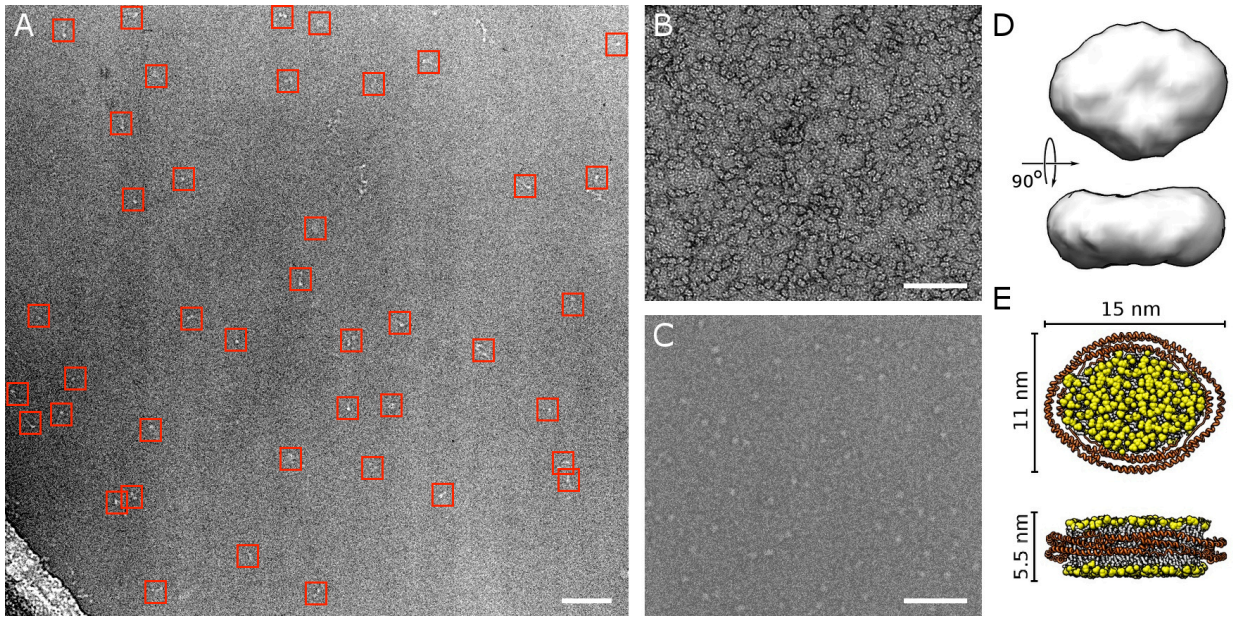

Figure S1: Original Micrographs A. Repesentative micrograph of integrins under near-physiological cryo-conditions. Integrins appear white. The boxes mark well-separated particles. A selection of particles and their assignments to conformations and orientations is shown in Figure 2 in the main text. **B.** Nanodiscs in negative stain showing a narrow size and shape distribution but tendency for preferred orientation (top view). **C.** Nanodiscs under near-physiological cryo-conditions also showing a narrow size and shape distribution but without the tendency of preferred orientation. **D.** Three-dimensional reconstruction of nanodiscs derived from cryo-data such as that shown in (C). No symmetry was applied. Note that the dimensions of the top view match well those seen in the negatively stained data (B). **E.** Model of nanodisc derived from the reconstruction in (D). The bars in (A-C) correspond to 100 nm.

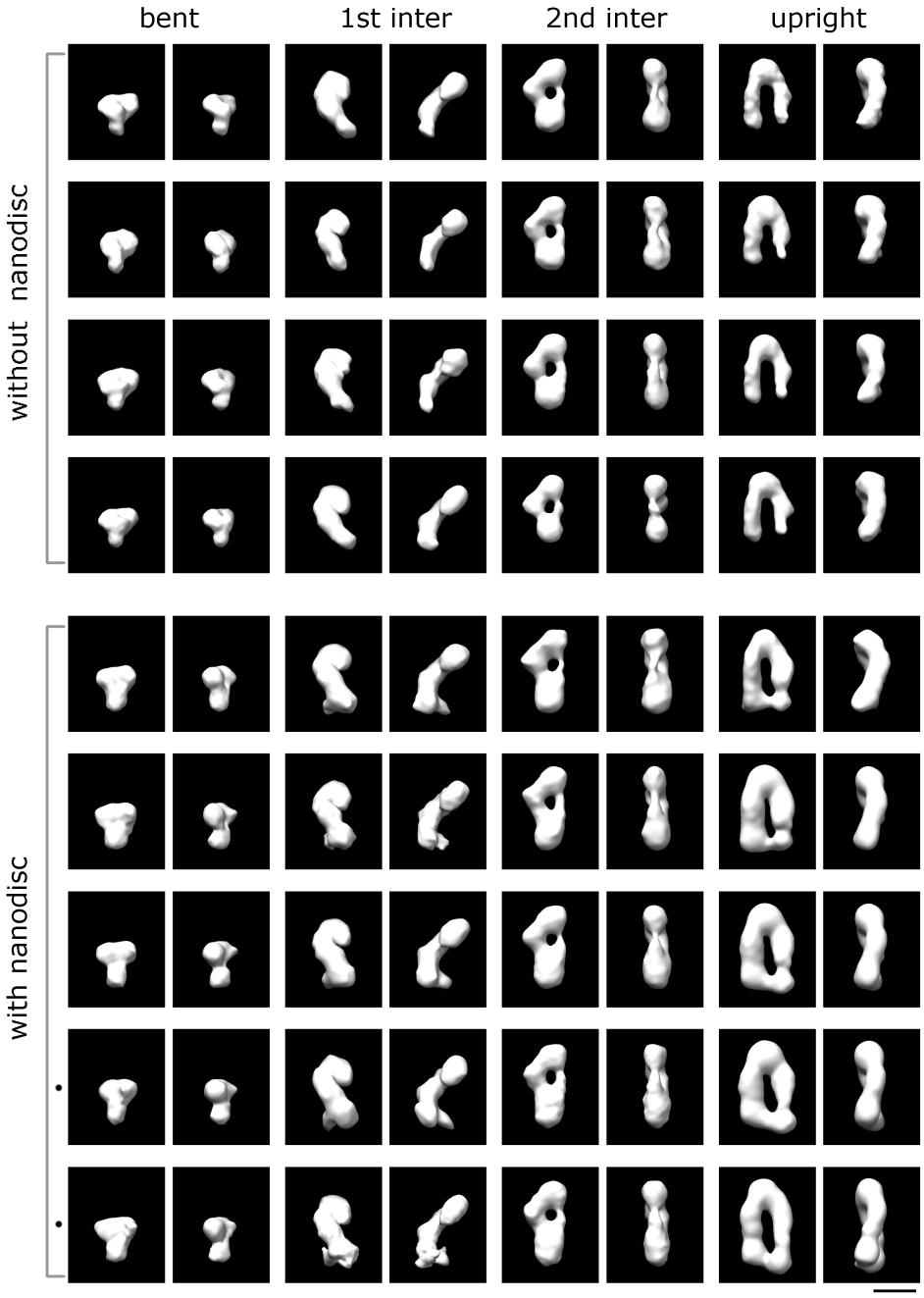

Figure S2: Three-dimensional cryo reconstructions of integrin receptors in nine conditions. Surface representations of orthogonal views of reconstructions derived from nine independent data sets of integrin or integrin in nanodiscs. The reconstructions were filtered to 4-nm resolution for easy comparison and were obtained after iterative sorting. Conditions marked with dots had talin head domain present in the sample. The bar corresponds to 10 nm.

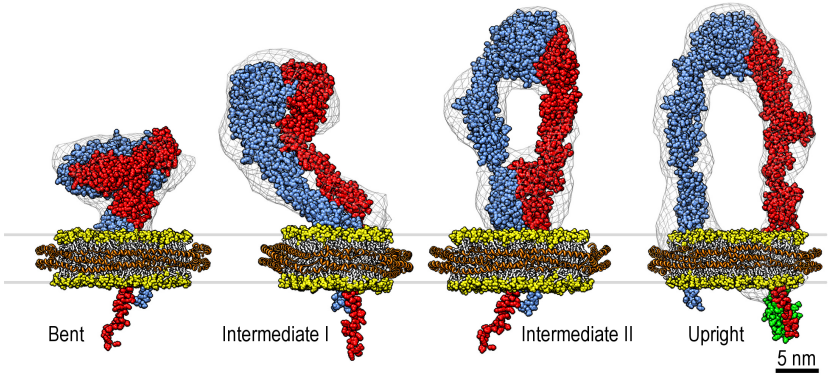

Figure S3: Space-filling models of the conformers in the conformational equilibrium of membrane-embedded integrins. The lipid bilayer of the nanodisc is shown with the head groups in yellow and the hydrophobic tails in white. Integrin (red: β-chain and blue: α-chain) and talin F3 (green) are also shown in space-filling representation. The protein belt of the nanodisc (orange) is shown in cartoon representation.

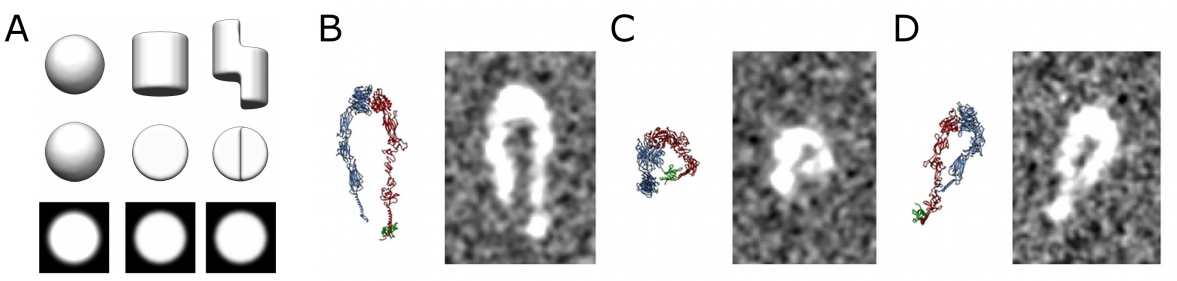

Figure S4: Ambiguities of two-dimensional projections. A. Very different three-dimensional structures (top rows) can yield indistinguishable two-dimensional projections (bottom row) **B-D.** The same three-dimensional structure can give rise to multiple two-dimensional projections. Depending on its orientation, the upright integrin conformation with separated legs (A) can also give rise to 2D projections that appear as a nodular, compact particle (C) or an upright conformation with closed legs (D).

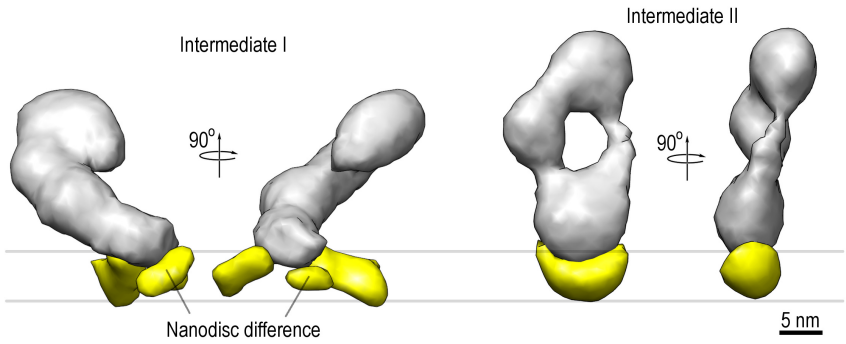

Figure S5: Nanodisc identification by difference mapping for intermediate conformations. A, B. Difference mapping of first (A) and second (B) intermediate conformations using reconstructions of integrin in the presence and absence of nanodiscs. Grey represents the density of integrin in the absence of nanodiscs, yellow the difference between integrin with nanodiscs minus integrin without nanodiscs,